Leila Hoseini and Azar Bagheri*

Catalytic properties of plate-like cadmium oxide nanoparticles in removal of sulfathiazole with anticancer activity

https://doi.org/10.1515/mgmc-2018-0025
Received May 30, 2018; accepted July 4, 2018

Abstract: The study of the interaction of drugs with DNA is very exciting and significant not only for understanding the mechanism of the interaction but also for the design of new drugs. Here, we report the results of Fourier transform infrared (FT-IR) and ultraviolet (UV)-visible spectroscopy studies to determine the external binding modes of sulfathiazole (STZ), and the binding constant and stability of the STZ-DNA complex in aqueous solution. The results of absorption spectra showed that the interaction of STZ-DNA is weak because there is only a hyperchromic effect. A hyperchromic effect reflects the corresponding changes of DNA in its conformation and structure after the drug-DNA interaction has occurred. Spectroscopic evidence revealed that STZ binds DNA with an overall binding constant of K (STZ-DNA) = 0.42×10^3 M^{-1}. FT-IR spectroscopy showed that the complexation of STZ with DNA occurred via A-T and PO_2 groups. Nano cadmium hydroxide has been synthesized using hexamine as the template at room temperature. Then, this nano cadmium hydroxide recrystallizes into nano cadmium oxide (CdO) at 400°C for 2 h. The product was characterized by using X-ray diffraction and scanning electron microscopy. The presence of drugs in aquatic media has emerged in the last decade as a new environmental risk. The other aim of this study was to investigate the degradation of the STZ antibiotic by nano-sized CdO under ultraviolet irradiation. Various experimental parameters, such as initial CdO concentration, initial pH, and reaction times, were investigated. According to the results, this method has a good performance in the removal of STZ.

Keywords: binding constant; cadmium oxide; DNA; hexamine; removal; sulfathiazole.

***Corresponding author: Azar Bagheri,** Department of Chemistry, Islamic Azad University, Center Tehran Branch, Tehran 11468, Iran, e-mail: Azar.bagheri@iauctb.ac.ir
Leila Hoseini: Department of Chemistry, Islamic Azad University, Center Tehran Branch, Tehran 11468, Iran

Introduction

Studies on the binding of small molecules to DNA are very important in the development of DNA molecular probes and new therapeutic reagents (Mrksich and Dervan, 1993). Interactions between small molecules and DNA can cause damage to cancer cells, blocking their division and resulting in cell death (Zuber et al., 1998; Chauhan et al., 2007; Arjmand et al., 2012). Small molecules can react with DNA via covalent or non-covalent interactions, with interest generally focusing on the latter. The binding of small molecules to DNA involves electrostatic interaction, intercalation between base pairs, and minor and major DNA grooves binding interaction (Rauf et al., 2005). The covalent mode of drug-DNA binding is irreversible and invariably causes the complete inhibition of DNA processes and subsequent cell death. The non-covalent mode of drug-DNA binding is further classified into three types: intercalation, groove binding, and external binding (Rauf et al., 2005). Minor groove binding drugs typically have several aromatic rings, such as pyrrole, furan, or benzene, connected by bonds possessing torsional freedom. Some ligands are also capable of forming non-specific, outside edge stacking interactions with the DNA phosphate backbone (external binding). Various techniques that are used to study the binding of drug molecules with DNA includes infrared (IR), Raman, circular dichroism, ultraviolet (UV)-visible, and nuclear magnetic resonance spectroscopies. The sulfonamide drugs are the first effective chemotherapeutic agents to be employed systemically for the prevention and cure of bacterial infection in human beings (Bhusari et al., 2000; Bhusare et al., 2001; Chandra and Roy, 2001; Ahmed et al., 2003; Horab et al., 2010). For this reason, sulfonamides occupy a unique position in the drug industry. The sulfonyl group plays a very important role as a key constituent of a number of biologically active molecules. Sulfathiazole (STZ) is a semisynthetic derivative of sulfa drug that exhibits antibacterial effects and antitumor activities in several cancer cell lines (Onoda et al., 2006; Son et al., 2009). In our laboratory, we have focused our attention to drugs and their metal complexes that target cellular DNA, to understand the mechanism

of action at the molecular level. Therefore, in this study, we report the results of Fourier transform (FT)-IR and UV-visible spectroscopic analysis of DNA interaction with STZ in aqueous solution at physiological conditions, using constant DNA concentration and various ligand/DNA(P) ratios of 1:120–1:10. Drug-DNA interactions can be studied by comparison of UV-visible absorption spectra of the free DNA and drug-DNA complexes, which are usually different. Compounds binding with DNA through intercalation with strong interaction usually results in hypochromism and bathochromism (Bauer and Vinograd, 1970; Neidle and Abraham, 1984; Keck and Lippard, 1992; Moucheron and Kirsch-Mesmaeker, 1998). The hyperchromic effect is the outstanding increase in absorbance of DNA upon denaturation.

Over the past few years, antibiotics have been considered emerging pollutants due to their continuous input and persistence in the aquatic ecosystem even at low concentrations. Adverse effects have also been demonstrated for sulfonamides, a family of antibiotics commonly used in cattle-rearing facilities and also in human medicine. Sulfonamides have been detected in basically all kinds of environmental water matrices (Göbel et al., 2005, 2007; García-Galán et al., 2010, 2011). In urban ecosystems, wastewater treatment plants are considered to be the main entry pathways for sulfonamides and pharmaceuticals in general, and several works have been devoted to evaluating their presence and fate in influent and effluent wastewaters (Reemtsma et al., 2006; García-Galán et al., 2010; Gros et al., 2010). Few articles of antibiotics degradation were found.

In this study, the interactions of STZ with DNA in aqueous solution at physiological conditions were analyzed using spectroscopic methods. STZ complex with DNA was identified, and the effects of STZ complexation on nucleic acid conformation, aggregation, and particle formation are discussed here. Because of the appropriate optical and electrical properties, cadmium oxide (CdO) nanostructures are used in solar cells, gas sensors, transparent electrodes, photodiodes, catalysts, and optoelectronic devices (Liu et al., 2003; Mane et al., 2006; Sarma and Tao, 2007; Salunkhe and Lokhande, 2008; Kim and Kwon, 2009; Li et al., 2009; Yakuphanoglu, 2010; Yakuphanoglu et al., 2010; Pawar et al., 2011). Therefore, the other objective of the present study was to evaluate STZ degradation by UV irradiation, UV/CdO.

Results and discussion

Absorption spectra of the STZ-DNA complex

UV-visible absorption spectroscopy is simple, widely used, and one of the most effective methods in detecting the interaction of small molecules with DNA. The UV-visible absorption spectrum of DNA shows a broad band in the UV region with a maximum absorption at 260 nm (Figure 1). With increasing concentrations of DNA to a fixed concentration of STZ, the absorption bands of the complex were affected, resulting in the tendency of hyperchromism. The UV results showed that STZ binds externally to DNA. The increase in intensity of STZ characteristic UV-visible band is due to drug-DNA interaction at the DNA surface (Freifelder, 1976; Lambert et al., 1998; Kumar et al., 2009). Based on the variation in absorbance,

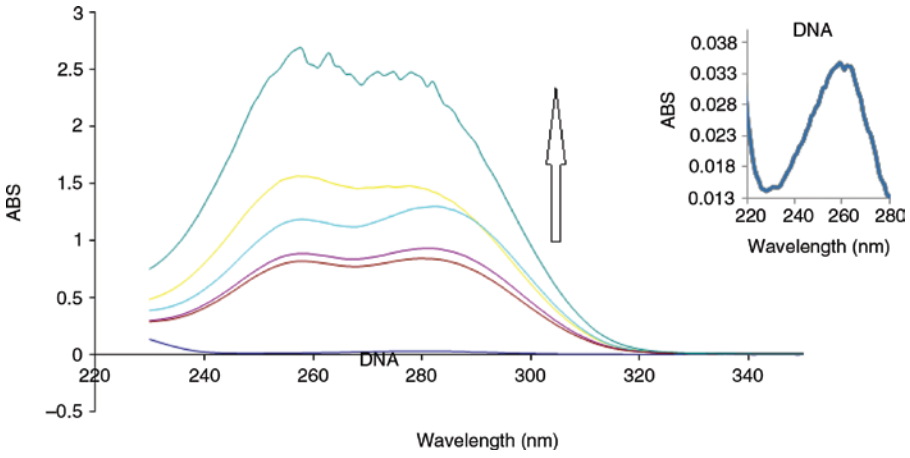

Figure 1: UV-visible spectra characteristics of STZ and their DNA adducts, with constant STZ concentration of 2.5 mM and different DNA concentrations of 0.5–2.5 mM.
The arrow indicates increasing concentrations of DNA.

the intrinsic binding constant/association constant (K) of the drug with DNA can be determined according to the Benesi-Hildebrand equation (Benesi and Hildebrand, 1949). The calculations of the overall binding constants were carried out using UV spectroscopy, as reported previously (Andrushchenko et al., 2002; Poluyanichko et al., 2004). The equilibrium for each ligand and DNA complex was established as follows:

$$\text{Ligand} + \text{DNA} \Leftrightarrow \text{ligand:DNA}.$$
$$K = [\text{ligand:DNA}]/[\text{ligand}][\text{DNA}].$$

The double reciprocal plot of $1/[A - A_0]$ vs. $1/[\text{drug}]$ is linear, and the association binding constant (K) is calculated from the ratio of the intercept on the vertical coordinate axis to the slope (Stephanos et al., 1996; (Zhong et al., 2004) (Figure 2), where A_0 is the initial absorption of DNA (260 nm) and A is the recorded absorption at different STZ concentrations (l). Therefore, the overall binding constants are estimated to be K for (STZ-DNA) = 0.42×10^3 M^{-1}.

FT-IR spectra STZ-DNA complexes

The FT-IR difference spectra [(DNA solution + drug solution) – (DNA solution)] were produced, using the band at 968 cm^{-1} as internal reference. This band is due to the sugar C-C stretching modes and shows no spectral changes upon drug complexation. The intensity ratio variations of several DNA in-plane vibrations related to A-T and G-C base pairs as well as the backbone PO_2 stretching were measured with respect to the reference band at 968 cm^{-1} as a function of drug concentrations with an error of ±3%. These intensity ratios were used to determine drug binding to DNA bases or the backbone phosphate groups (Neault and Tajmir-Riahi, 1996, 1998; Ahmed-Ouameur and Tajmir-Riahi, 2004; Ahmed-Ouameur et al., 2005). In this work, FT-IR spectroscopy has been employed to study the interactions of STZ with DNA. The FT-IR spectra of STZ-DNA complexes between 1800 and 600 cm^{-1} are presented in Figure 3. The spectral changes (intensity and shifting) of several prominent DNA in-plane vibrations at 1715 cm^{-1} (G), 1667 cm^{-1} (T), 1607 cm^{-1} (A), 1527 cm^{-1} (C), and 1225 cm^{-1} (PO_2 asymmetric stretch) were monitored (Theophanides, 1981; Alvi et al., 1986; Hoffmann et al., 1995; Tajmir-Riahi et al., 1996; Khorasani-Motlagh et al., 2011; Zermeño et al., 2011). At different STZ concentrations, helix stabilization and conformational change occurred upon the interaction of STZ with DNA. Evidence for this comes from the changes in intensity and shifting of the

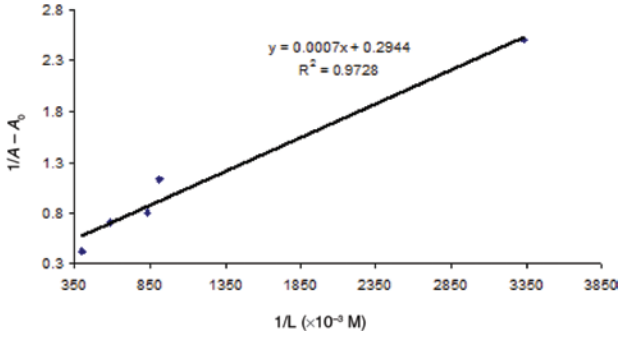

Figure 2: Plot of $1/(A - A_0)$ vs. $1/[\text{STZ}]$, for the determination of binding constants of STZ-DNA adducts.
Different DNA absorbances: 0.728, 0.874, 1.155, 1.599, and 2.675.

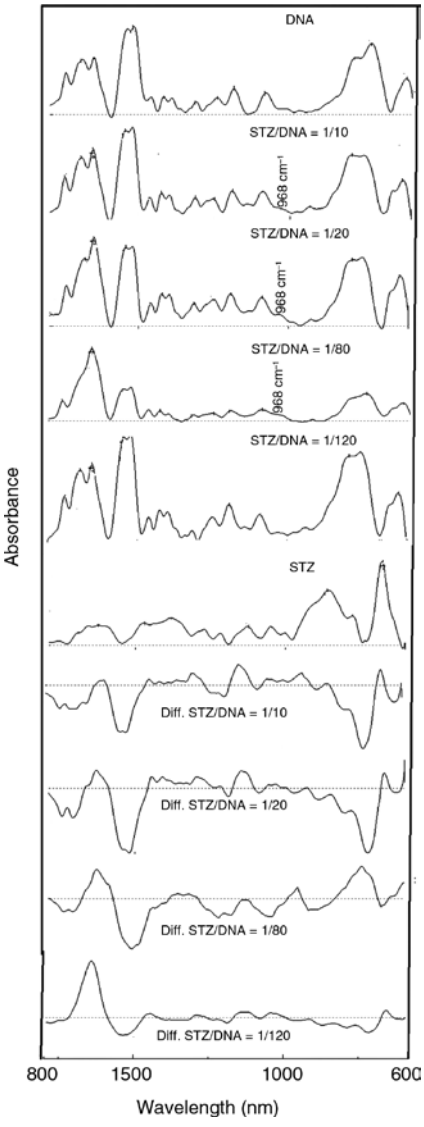

Figure 3: FT-IR spectra of the free calf thymus DNA-STZ complexes at different molar ratios in the region of 1800–600 cm^{-1} in aqueous solution.

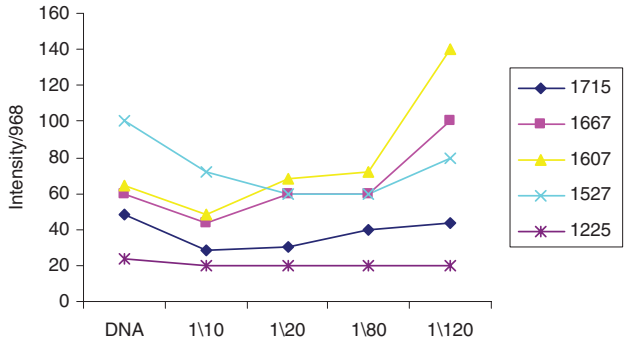

Figure 4: Intensity ratio variations for DNA in-plane vibrations as a function of STZ concentrations (0.05–12.5 mM).
Intensity ratios for the DNA bands at 1715 (G), 1667 (T), 1607 (A), 1527 (C), and 1225 (PO_2 asymmetric) referenced to the DNA band at 968 cm^{-1}.

absorption bands in the region of 1800–1550 cm^{-1} due to the in-plane DNA. At low STZ concentrations, an intensity increase in difference spectra of STZ-DNA was observed at 1607 and 1667 cm^{-1} (Figures 3 and 4). The intensity increase of the bases can be related to destabilization of DNA helix upon STZ interaction. Major shifting was observed for the thymine and guanine bands at 1667–1715 cm^{-1}, which can be related to major interaction of STZ with T and G in drug at different concentrations. Decrease in intensity of DNA vibrations was observed as a result of STZ-phosphate interaction. There was no evident shift of PO_2 stretching, while the intensity of absorptions changed (Figure 4).

Structural investigations

The X-ray diffraction (XRD) pattern of CdO is shown in Figure 5. This pattern clearly confirmed the presence of the CdO phase. The diffraction peaks at 2θ values of 32.90°, 38.20°, 55.20°, 65.80°, and 69.20° matching with the 111, 200, 220, 311, and 222 of cubic CdO (JCPDS 05-0640) indicated the formation of this compound. The average crystallite size (D) of the calcined CdO nanoparticle was estimated from the full width at half maximum of the diffraction peaks using Debye-Scherrer's method. The average crystallite size in calcined CdO was 59 nm. The surface morphologies of the CdO were studied using scanning electron microscopy (SEM), as shown in Figure 6.

Degradation of STZ and removal under different oxidation systems

The efficiency of the UV/CdO photocatalytic process to remove STZ from aqueous solution was investigated in the presence of CdO. To determine the photocatalyst effect, two experiments with and without a catalyst were made. The results of STZ degradation and removal under the optimum conditions by different systems at an initial STZ concentration of 30 mgL^{-1} are shown in Figure 7.

Influence of CdO concentrations on STZ degradation

To investigate the effect of CdO concentration on photocatalytic efficiency, a set of experiments were done at pH 11 with different CdO concentrations at a range of 0.2–1.4 gL^{-1}. The results showed that the optimum concentration of CdO catalyst was 1.1 gL^{-1} (Figure 8).

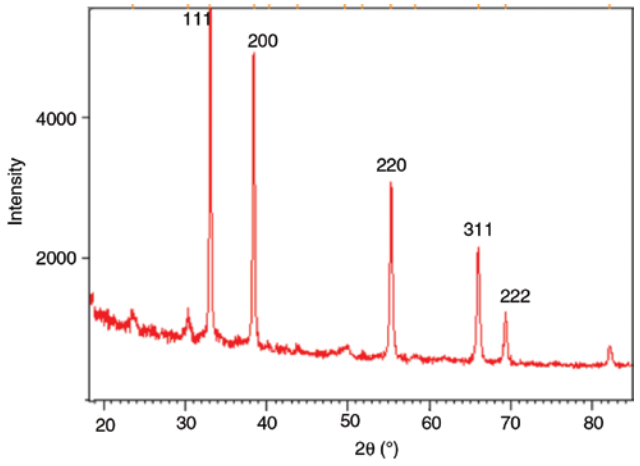

Figure 5: XRD pattern of CdO nanoparticles.

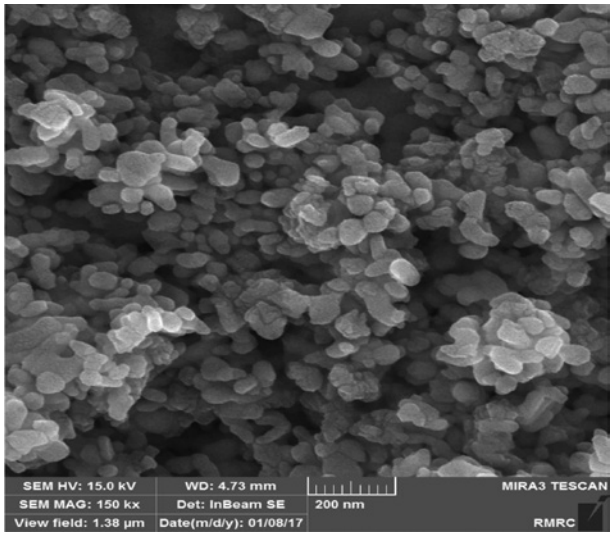

Figure 6: SEM image of CdO nanoparticles.

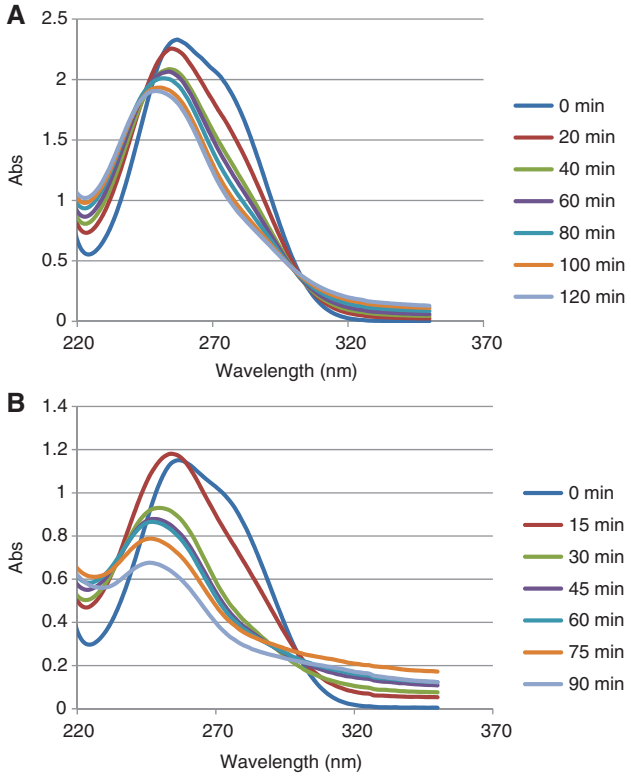

Figure 7: Changes of UV-visible spectra of 30 mgL^{-1} aqueous solution of STZ in optimum conditions, during the photocatalytic process of UV/CdO with irradiation time of 0–120 and 0–90 min (A) without catalyst and (B) with catalyst, respectively.

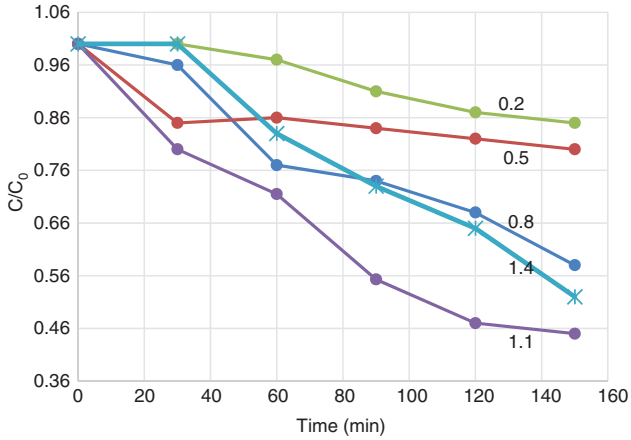

Figure 8: Influence of a various concentrations of CdO on STZ degradation ([STZ] = 30 mgL^{-1}, pH 11).

Influence of initial pH on STZ degradation

To evaluate the influence of initial pH on the removal efficiency, the pH of the solution was adjusted at the range of 3–11 (Figures 9 and 10). The minimum of degradation was recorded at pH 7 and increased with acidic as well as alkaline pH values. Enforcement of the degradation rate under alkaline condition could be attributed to the increase of hydroxyl ions, which induces more hydroxyl radical formation. In the acidic condition, it can also be due to the presence of the ion sulfate when the initial pH is adjusted to 3, as this anion can act as a hydroxyl scavenger and can compete with the molecules for the photon of the system. Thus, an increase or decrease in pH from neutral value increases the rate of degradation.

Conclusions

Spectral changes were observed in the spectra of drug-DNA complexes in which loss of intensity of the DNA in-plane vibrations was attributed to partial helix stabilization, while the increase in intensity of DNA vibrations was attributed to some degree of helix destabilization. The intensity variations for the bases and PO_2 bands are characterized by strong positive and negative features around 1000–1800 cm^{-1} in the difference spectra of STZ-DNA. In the difference spectra of STZ-DNA complexes, positive features at 1667, 1607, and 1225 cm^{-1} are due to binding of STZ to adenine N7, thymine O_2, and backbone PO_2 groups (Figures 3 and 4). Interaction of calf thymus DNA with STZ in aqueous solution has shown binding to DNA bases. Binding to guanine N7 occurs at the early stage of helix destabilization. A similar feature was observed for carboplatin, a platinum anticancer drug. Under the experimental condition, the binding to PO_2 is typically electrostatic in nature. In our study, UV-visible spectroscopy showed that the interaction of STZ-DNA is weak (i.e. electrostatic or groove binding) because a shift is not observed.

Heterogeneous photocatalysis provides a cheap and effective alternative to clean water production and environmental remediation. In this study, it has been shown that the presence of CdO in the UV/CdO photocatalysis system had a positive influence in terms of faster degradation of STZ. As one can observe in Figure 7, a photolysis degradation can be negligible in the overall degradation process. Under UV irradiation, the degradation of STZ was <15% within 2 h at the initial STZ concentration of 30 mg L^{-1} and at natural pH of 11. The degradation was mainly due to the active species (hydroxyl radicals) produced during the photocatalytic process. Important points in the semiconductor photocatalyst materials are the width of the band gap and levels of the conduction and valence bands. The degradation rates are also influenced by pH. In general, a higher degradation extent would be expected that occurs at strong basic pH values because of the presence of more hydroxyl anions in the solution. At acidic

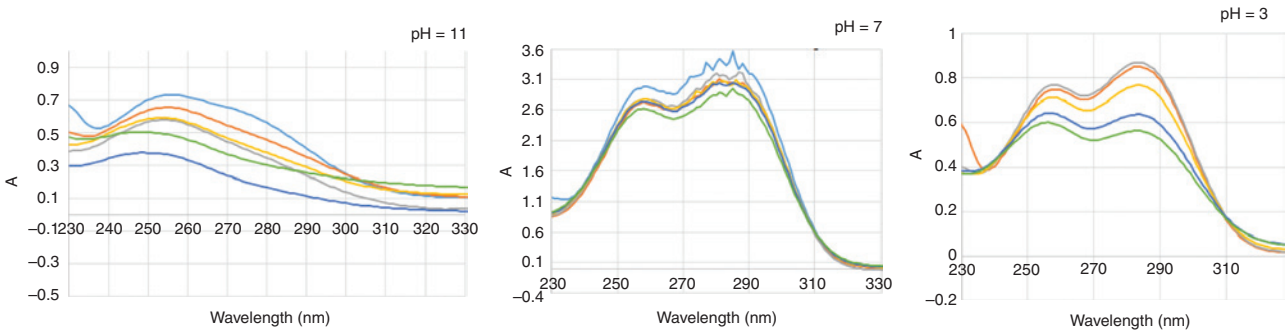

Figure 9: Changes of UV-visible spectra of 30 mgL^{-1} aqueous solution of STZ in various pH values during the photocatalytic process of UV/CdO with an irradiation time of 0–90 min.

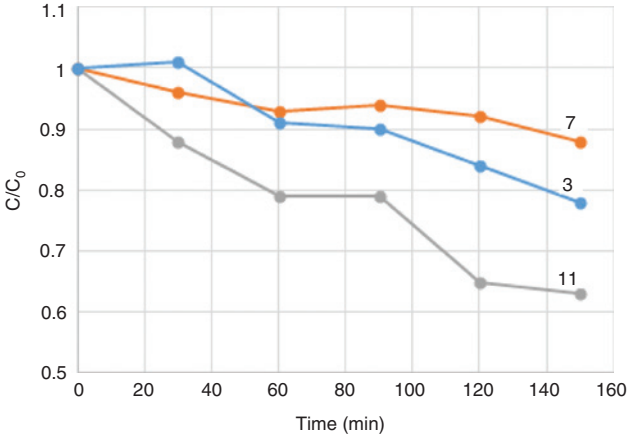

Figure 10: Influence of various pH values on STZ degradation ([STZ] = 30 mgL^{-1} and [CdO] = 1.1 mgL^{-1}).

pH, the sulfur atom in the sulfonamide molecule could be mineralized to SO_4^{2-}, whereas the nitrogen of the molecule could be mineralized either to NH_3 or to NO_2^- and/or NO_3^- (Calza et al., 2004), and these anions can give rise to a gradual pH decrease, as long as the molecule is degraded. Thus, it seems that the charge of both CdO surface and STZ do not influence the STZ degradation.

Experimental section

Apparatus

For the UV/photocatalyst process, irradiation was performed in a batch photoreactor with two mercury lamps, Philips 8W (UV-C). A magnetic stirrer was used to ensure complete mixing in the tank (stirring speed = 250 rpm). A Shimadzu 2101 UV-visible spectrophotometer (Shimadzu, Columbia, MD, USA) was employed for absorbance measurements using silica cells with a 10-mm path length. IR spectra were recorded on a Jasco FT-IR spectrometer (JASCO Corporation, Hachiojishi, Tokyo, Japan) equipped with a liquid-nitrogen-cooled HgCdTe (MCT) detector and a KBr beam splitter. The spectra of the STZ-DNA solutions were acquired using a cell assembled with AgBr windows. The morphology of nanostructured CdO was determined by SEM on a Holland Philips XL30 microscope (Holland, The Netherlands). XRD analysis was carried out at room temperature using a Holland Philips Xpert X-ray powder diffractometer (Holland, The Netherlands) with CuKα radiation (λ = 0.15406 nm), over the 2θ collection range 0–80°.

Materials

Calf thymus DNA, cadmium acetate, and STZ were purchased from Sigma Chemical Company. Other chemicals were purchased from Merck. All chemicals used were analytic-grade reagents without any further purification.

Degradation experiments

For the photodegradation of STZ, a solution containing a known concentration of drug and photocatalyst were prepared and allowed to equilibrate for 30 min in darkness. The suspension pH values were adjusted at the desired level using dilute NaOH and H_2SO_4 (the pH values were measured with a Horiba D-14 pH meter). The photodegradation reaction took place under the radiation of a mercury lamp, while agitation was maintained to keep the suspension homogeneous. The concentration of the samples was determined using a UV-visible spectrophotometer. The degree of photodegradation as a function of time is given by

$$\text{Removal efficiency} = \frac{C_0 - C_t}{C_0} \times 100\%, \quad (1)$$

where C_0 and C_t are the concentration of STZ at $t = 0$ and t, respectively.

Preparation of stock solutions

Sodium-DNA (5 $mg{\cdot}mL^{-1}$) was dissolved in distilled water (pH 7) at 5°C for 24 h with occasional stirring to ensure the formation of a homogeneous solution. The UV absorbance at 260 nm of a diluted

solution (1/250) of calf thymus DNA used in our experiments was 0.661 (path length was 1 cm), and the final concentration of the DNA solution was 12.5 mM in DNA phosphate. The appropriate amounts of STZ (0.05–12.5 mM) were prepared in distilled water and added dropwise to DNA solution in order to attain the desired ligand/DNA(P) molar ratios (*r*) of 1:120, 1:80, 1:20, and 1:10 with a final DNA(P) concentration of 6.25 mM (path length was 0.03 cm). The pH of the solutions was adjusted at 7.0 ± 0.2 using NaOH solution.

Synthesis of CdO

In a typical experimental procedure, $Cd(CH_3COO)_2 \cdot 2H_2O$ was dissolved in distilled water to form a 0.5 M solution. The precursor solution obtained (4 mL) was added to a 100 mL conical flask containing 1.21 g of hexamine and sodium hydroxide (0.07 mol) under magnetic stirring. The resulting solution was placed at room temperature for 2 days. After each synthesis, white crystalline products were collected by centrifugation, and washed with distilled water and ethanol several times. Then, the resulting precipitate was collected by centrifugation and washed several times with water and ethanol. The cadmium hydroxide precipitate was obtained, placed in a vacuum oven at a temperature 60°C for 12 h, and then placed in the furnace for 2 h at 420°C and converted to CdO. Then, to ensure the formation of nanoparticles, the XRD pattern was taken.

Acknowledgments: We wish to thank the Islamic Azad University Center Tehran Branch for its invaluable support through the project.

References

Ahmed, B.; Khan, S. A.; Alam, T. Synthesis and antihepatotoxic activity of some heterocyclic compounds containing the 1,4-dioxane ring system. *Pharmazie* **2003**, *58*, 173–176.

Ahmed-Ouameur, A.; Tajmir-Riahi, H. A. Structural analysis of DNA interactions with biogenic polyamines and cobalt(III)hexamine studied by Fourier transform infrared and capillary electrophoresis. *J. Biol. Chem.* **2004**, *279*, 42041–42054.

Ahmed-Ouameur, A.; Marty, R.; Tajmir-Riahi, H. A. Human serum albumin complexes with chlorophyll and chlorohyllin. *Biopolymers* **2005**, *77*, 129–136.

Alvi, N.; Rizi, R. Y.; Hadi, S. M. Interaction of quercetin with DNA. *Biosci. Rep.* **1986**, *6*, 861–868.

Andrushchenko, V. V.; Leonenko, Z.; van de Sande, H.; Wieser, H. Vibrational CD (VCD) and atomic force microscopy (AFM) study of DNA interaction with Cr^{3+} ions: VCD and AFM evidence of DNA condensation. *Biopolymers* **2002**, *61*, 243–248.

Arjmand, F.; Parveen, S.; Afzal, M.; Toupet, L.; Ben Hadda, T. Molecular drug design, synthesis and crystal structure determination of Cu^{II}-Sn^{IV} heterobimetallic core: DNA binding and cleavage studies. *Eur. J. Med. Chem*. **2012**, *49*, 141–150.

Bauer, W.; Vinograd, J. The interaction of closed circular DNA with intercalative dyes: III. Dependence of the buoyant density upon superhelix density and base composition. *J. Mol. Biol.* **1970**, *54*, 281–298.

Benesi, H. A.; Hildebrand, J. H. Spectrophotometric investigation of the interaction of iodine with aromatic hydrocarbons, *J. Am. Chem. Soc*. **1949**, *71*, 2703–2707.

Bhusare, S. R.; Pawar, R. P.; Vibhute, Y. B. Synthesis and antibacterial activity of some new 2-(substituted phenyl sulfonamido)-6-substituted benzothiazoles. *Indian J. Heterocyclic Chem*. **2001**, *11*, 78–80.

Bhusari, K. P.; Khedekar, P. B.; Umathe, S. N.; Bahekar, R. H.; Raghu, A. Synthesis of 8-bromo-9-substituted-1,3-benzothiazolo-[5,1-b]-1, 3, 4-triazoles and their anthelmintic activity. *Indian J. Heterocyclic Chem*. **2000**, *9*, 275–278.

Calza, P.; Medana, C.; Pazzi, M.; Baiocchi, C.; Pelizzetti, E. Photocatalytic transformations of sulphonamides on titanium dioxide. *Appl. Catal. B: Environ*. **2004**, *53*, 63–69.

Chandra, B.; Roy, K. Synthesis of some new p-toluene sulfonamido glutaramides. *Indian J. Heterocyclic Chem.* **2001**, *10*, 237–238.

Chauhan, M.; Banerjee, K.; Arjmand, F. DNA binding studies of novel copper(II) complexes containing L-tryptophan as chiral auxiliary: *in vitro* antitumor activity of Cu-Sn_2 complex in human neuroblastoma cells. *Inorg. Chem*. **2007**, *46*, 3072–3082.

Freifelder, D. Physical Biochemistry; W.H. Freeman and Company: New York, 1976, Chapter 15.

García-Galán, M. J.; Díaz-Cruz, M. S.; Barceló, D. Determination of 19 sulfonamides in environmental water samples by automated on-line solid-phase extraction-liquid chromatography-tandem mass spectrometry (SPE-LC-MS/MS). *Talanta* **2010**, *81*, 355–366.

García-Galán, M. J.; Díaz-Cruz, M. S.; Barceló, D. Occurrence of sulfonamide residues along the Ebro river basin: removal in wastewater treatment plants and environmental impact assessment. *Environ. Int*. **2011**, *37*, 462–473.

Göbel, A.; Thomsen, A.; McArdell, C. S.; Joss, A.; Giger, W. Occurrence and sorption behavior of sulfonamides, macrolides, and trimethoprim in activated sludge treatment. *Environ. Sci. Technol*. **2005**, *39*, 3981–3989.

Göbel, A.; McArdell, C. S.; Joss, A.; Siegrist, H.; Giger, W. Fate of sulfonamides, macrolides, and trimethoprim in different wastewater treatment technologies. *Sci. Total Environ.* **2007**, *372*, 361–371.

Gros, M.; Petrovic, M.; Ginebreda, A.; Barceló, D. Removal of pharmaceuticals during wastewater treatment and environmental risk assessment using hazard indexes. *Environ. Int.* **2010**, *36*, 15–26.

Hoffmann, M. R.; Martin, S. T.; Choi, W. Y.; Bahnemann, D. W. Environmental applications of semiconductor photocatalysis. *Chem. Rev*. **1995**, *95*, 69–96.

Horab, M. M.; Ragab, F. A.; Heiba, H. I.; Arafa, R. K. *In vitro* anticancer screening and radiosensitizing evaluation of some new quinolines and pyrimido[4,5-b]quinolines bearing a sulfonamide moiety. *Eur. J. Med. Chem*. **2010**, *45*, 3677–3684.

Keck, M. V.; Lippard, S. J. Unwinding of supercoiled DNA by platinum-ethidium and related complexes. *J. Am. Chem. Soc.* **1992**, *114*, 3386–3390.

Khorasani-Motlagh, M.; Noroozifar, M.; Khmmarnia, S. Study on fluorescence and DNA-binding of praseodymium (III) complex containing 2,2'-bipyridine. *Spectrochim. Acta A* **2011**, *78*, 389–395.

Kim, M. H.; Kwon, Y. U. Semiconductor CdO as a blocking layer material on DSSC electrode: mechanism and application. *J. Phys. Chem. C* **2009**, *113*, 17176–17182.

Kumar, K. A.; Reddy, K. L.; Vidhisha, S.; Satyanarayana, S. Synthesis, characterization and DNA binding and photocleavage studies of [Ru(bpy)2BDPPZ]2+, [Ru(dmb)2BDPPZ]2+ and [Ru(phen)2BDPPZ]2+ complexes and their antimicrobial activity. *Appl. Organometal. Chem*. **2009**, *23*, 409–420.

Lambert, J. B.; Shurvell, H. F.; Lightner, D. A.; Cooks, R. G. Organic Structural Spectroscopy; Prentice-Hall Inc.: Hillsdale, NJ, 1998, Chapters 10–11.

Li, J.; Ni, Y.; Liu, J.; Hong, J. Preparation, conversion, and comparison of the photocatalytic property of Cd(OH)2, CdO. CdS and CdSe. *J. Phys. Chem. Solid* **2009**, *70*, 1285–1289.

Liu, X.; Li, C.; Han, S.; Han, J.; Zhou, C. Synthesis and electronic transport studies of CdO nanoneedles. *Appl. Phys. Lett.* **2003**, *82*, 1950–1952.

Mane, R. S.; Pathan, H. M.; Lokhande, C. D.; Han, S. H. An effective use of nanocrystalline CdO thin films in dye-sensitized solar cells. *Sol. Energy* **2006**, 80, 185–190.

Moucheron, C.; Kirsch-Mesmaeker, A. New DNA-binding ruthenium(II) complexes as photo-reagents for mononucleotides and DNA. *J. Phys. Org. Chem*. **1998**, *11*, 577–583.

Mrksich, M.; Dervan, P. B. Antiparallel side-by-side heterodimer for sequence-specific recognition in the minor groove of DNA by a distamycin/1-methylimidazole-2-carboxamide-netropsin pair. *J. Am. Chem. Soc*. **1993**, *115*, 2572–2576.

Neault, F.; Tajmir-Riahi, H. A. Diethylstilbestrol-DNA interaction studied by Fourier transform infrared and Raman spectroscopy. *J. Biol. Chem*. **1996**, *271*, 8140–8143.

Neault, F.; Tajmir-Riahi, H. A. DNA-chlorophyllin interaction. *J. Phys. Chem. B*. **1998**, *102*, 1610–1614.

Neidle, S.; Abraham, Z. Structural and sequence-dependent aspects of drug intercalation into nucleic acid. *Crit. Rev. Biochem*. **1984**, *171*, 73–121.

Onoda, T.; Ono, T.; Dhar, D. K.; Yamanoi, A.; Nagasue, N. Tetracycline analogues (sulfathiazole and COL-3) induce caspase-dependent and -independent apoptosis in human colon cancer cells. *Int. J. Cancer.* **2006**, *118*, 1309–1315.

Pawar, S. M.; Pawar, B. S.; Kim, J. H.; Joo, O. S.; Lokhande, C. D. Recent status of chemical bath deposited metal chalcogenide and metal oxide thin films. *Curr. Appl. Phys* **2011**, *11*, 117–161.

Poluyanichko, A. M.; Andrushchenko, V. V.; Chikhirzhina, V. I.; Vorob'eb, E. V.; Wieser, H. The effect of manganese(II) on DNA structure: electronic and vibrational circular dichroism studies. *Nucleic Acids Res*. **2004**, *32*, 989.

Rauf, S.; Gooding, J. J.; Akhtar, K.; Ghauri, M. A.; Rahman, M.; Anwar, M. A.; Khalid, A. M. Electrochemical approach of anticancer drugs-DNA interaction. *J. Pharmaceut. Biomed. Anal.* **2005**, *37*, 205–217.

Reemtsma, T.; Weiss, S.; Mueller, J.; Petrovic, M.; González, S.; Barcelo, D.; Ventura, F.; Knepper, T. P. Polar pollutants entry into the water cycle by municipal wastewater: a European perspective. *Environ. Sci. Technol.* **2006**, *40*, 5451–5458.

Salunkhe, R. R.; Lokhande, C. D. Effect of film thickness on liquefied petroleum gas (LPG) sensing properties of SILAR deposited CdO thin films. *Sens. Actuat. B: Chem.* **2008**, *129*, 345–351.

Sarma, T. V. S.; Tao, S. An active core fiber optic sensor for detecting trace H_2S at high temperature using a cadmium oxide doped porous silica optical fiber as a transducer. *Sens. Actuat. B: Chem.* **2007**, *127*, 471–479.

Son, K.; Fujioka, S.; Iida, T.; Furukawa, K.; Fujita, T.; Yamada, H.; Chiao, P. J.; Yanaga, K. Doxycycline induces apoptosis in PANC-1 pancreatic cancer cells. *Anticancer Res*. **2009**, *29*, 3995–4003.

Stephanos, J. Drug-protein interactions: two-site binding of heterocyclic ligands to a monomeric hemoglobin. *J. Inorg. Biochem*. **1996**, *62*, 155–169.

Tajmir-Riahi, H. A.; Neault, J. F.; Naoui, M.; Diamantoglou, S. The effect of HCl on the solution structure of calf thymus DNA: a comparative study of DNA denaturation by proton and metal cations using Fourier transform IR difference spectroscopy. *Biopolymers* **1996**, *35*, 493–497.

Theophanides, T. Fourier transform infrared spectra of calf thymus DNA and its reactions with the anticancer drug cisplatin. *Appl. Spectrosc.* **1981**, *35*, 461–465.

Yakuphanoglu, F. Nanocluster n-CdO thin film by sol-gel for solar cell applications. *Appl. Surf. Sci.* **2010**, *257*, 1413–1419.

Yakuphanoglu, F.; Caglar, M.; Caglar, Y.; Ilican, S. Electrical characterization of nanocluster n-CdO/p-Si heterojunction diode. *J. Alloys Compd*. **2010**, *506*, 188–193.

Zermeño, B. B.; Moctezuma, E.; García-Alamilla, R. Photocatalytic degradation of phenol and 4-chlorophenol with titania, oxygen and ozone. *Sustain. Environ. Res*. **2011**, *21*, 299–305.

Zhong, W.; Wang, Y.; Yu, J. S.; Liang, Y.; Ni, K.; Tu, S. The interaction of human serum albumin with a novel antidiabetic agent – SU-118. *J. Pharm. Sci.* **2004**, *93*, 1039–1043.

Zuber, G.; Quada, J. C.; Hecht, S. M. Sequence selective cleavage of a DNA octanucleotide by chlorinated bithiazoles and bleomycins. *J. Am. Chem. Soc*. **1998**, *120*, 9368–9369.